ChemComm

COMMUNICATION

View Article Online
View Journal | View Issue

Cite this: *Chem. Commun.*, 2025, **61**, 17934

Received 15th August 2025,
Accepted 14th October 2025

DOI: 10.1039/d5cc04696c

rsc.li/chemcomm

Less is more? Probing the template amount required for solid-state olefin [2 + 2] photocycloaddition in a ball mill

Mario Pajić, Senada Muratović and Marina Juribašić Kulcsár *

The first template-assisted olefin [2 + 2] photocycloaddition performed in a ball mill is reported. Using catalytic amounts of template resorcinol (as low as 10 mol%) enables rapid, quantitative and stereoselective dimerisation of *trans*-1,2-bis(4-pyridyl)ethene. *In situ* Raman monitoring of the photomechanochemical reactions reveals sigmoidal reaction profiles for olefin consumption, which were analyzed using the Finke–Watzky and JMAK kinetic models.

One of the most extensively studied reactions involving reactive supramolecular assemblies is the template-assisted olefin photodimerization.[1,2] This long-known[3–6] [2 + 2] cycloaddition typically requires a pre-formed co-crystal of the olefin with a template, where the molecules are pre-aligned in the Schmidt orientation.[7] Conventional methodologies rely on irradiating these photoactive co-crystals, often with periodic pauses to manually mix the sample.[8–13] This human intervention limits scalability and reproducibility of the reaction.[3–5,9,10]

Resorcinol (**res**) derivatives are efficient templates for olefin photodimerisation.[3–13] Until now, **res**-assisted cycloaddition of olefins has been carried out using manual[10,11] or vortex[12,13] mixing. The lowest reported template loading to achieve near-quantitative yield was 10 mol%, but it required 80 hours of irradiation with intermittent mixing.[10] More recently, 50 mol% of a **res** derivative enabled dimerisation in just 30 minutes in the vortex.[13] Despite these advances, real-time monitoring of the solid-state reaction remains challenging.

Ball milling[14] has emerged as a sustainable alternative to conventional solution-based protocols[15,16] and has recently extended into the area of photochemistry.[17] Since the initial breakthroughs in 2017,[18,19] solid-state photochemical transformations under ball-milling conditions have become an exciting field of research.[20–24] Ball milling offers advantages such as reproducibility, solvent-free conditions, and the ability to monitor reactions in real time without interrupting milling by solid-state Raman spectroscopy.[14–16,25]

Ruđer Bošković Institute, Bijenička cesta 54, HR-10000 Zagreb, Croatia. E-mail: marina.juribasic@irb.hr

In this study, we report the first example of a template-assisted olefin [2 + 2] photocycloaddition performed in a ball mill. Using as little as 10 mol% of **res** as a supramolecular catalyst, *trans*-1,2-bis-(4-pyridyl)ethene (**bpe**) was quantitatively and stereoselectively converted to *rctt*-1,2,3,4-tetrakis(4-pyridyl)cyclobutane (**tpcb**) within 2 hours, without any need for manual workup (Scheme 1). The reported solid-state approach is fast and simpler than previously reported methods.[10–13] The reactions were monitored *in situ* using Raman spectroscopy. Conversion profiles for **bpe** in reactions with 10–50 mol% of **res** showed sigmoidal kinetics dependent on the template amount, with 25 mol% **res** yielding the fastest transformation. Kinetic analysis using the Finke–Watzky (FW) and the Johnson–Mehl–Avrami–Kolmogorov (JMAK) models[26] revealed how template loading influences the reaction dynamics.

The olefin **bpe** and the template **res** (10–100 mol% relative to **bpe**) were milled under simultaneous irradiation for 3 hours. Quantitative photodimerisation was confirmed by powder X-ray diffraction (PXRD) and ^{1}H NMR analysis of the crude reaction mixtures. Reactions with catalytic amounts of **res** (10–50 mol%)

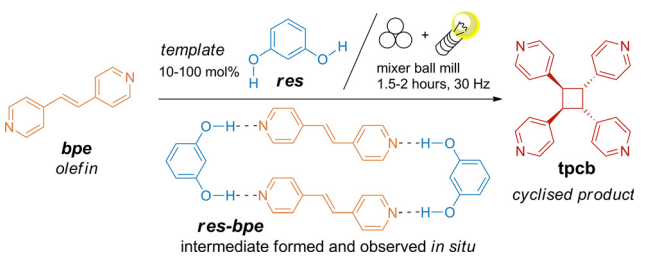

Scheme 1 The studied photo-mechanochemical olefin [2 + 2] cycloaddition. Ball-milling experiments were performed at ambient temperature controlled by air conditioner using an IST500 mixer mill with a built-in fan operating at 30 Hz. Reactions were conducted in 14 mL poly(methyl methacrylate) (PMMA) jars. One zirconium oxide (ZrO_2, 10 mm in diameter, 3.4 g) milling ball was used. The sample was irradiated by a module with five 365–367 nm light-emitting diodes (LEDs) (optical power 2–3 W). Distance of the LEDs from the jar was set to *ca.* 3 cm (Fig. S1). Heating of the LEDs and the jar during the reaction was modulated by a fan blowing between the jar and the LED module.

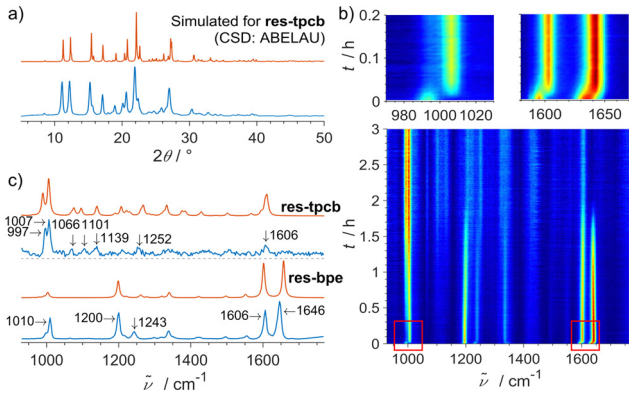

Fig. 1 Photo-mechanochemical reaction of **bpe** and **res** in a 1 : 1 molar ratio: (a) experimental (blue) and simulated (red) PXRD patterns of the obtained product **res-tpcb**, (b) 2D plot of the *in situ* Raman monitoring with insets showing fast formation of **res-bpe**, and (c) experimental (blue) and calculated (red) Raman spectra of **res-bpe** and **res-tpcb**. Raman experiments were performed following the previously described method[25] using a portable Raman system with the PD-LD (now Necsel) BlueBox laser source (785 nm excitation wavelength), equipped with the B&W-Tek fibre optic Raman BAC102 probe and coupled to the OceanOptics Maya2000-Pro spectrometer. Raman spectra were collected automatically for 8 seconds every 16 seconds, with a laser power of 400 mW and a probe distance of approx. 0.5 cm from the jar with a focus placed 1 mm inside the jar. For the reaction duration of 3 hours, 675 Raman spectra were collected.

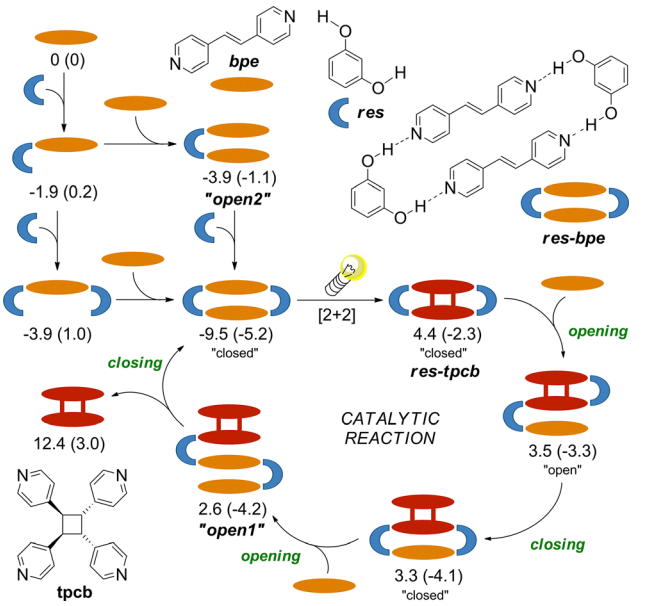

Fig. 2 Possible steps leading to the **res**-catalysed photodimerisation of **bpe**. Calculations were performed in the gas phase at B3LYP-D3(bj)/def2tzvp and ωB97X-D/def2tzvp (in parentheses) levels of theory using the programme package Gaussian16.[31] The reported free energies are in kcal mol^{-1} relative to reactants at 298.15 K and 1 atm without corrections. More details are listed in the SI.

proceeded faster than that with the equimolar **res**/**bpe** mixture, with 25 mol% **res** giving the fastest conversion. PXRD showed that the formed cyclobutane product **tpcb** was either unbound (CSD code: PYRBTA[27]) or part of a **res-tpcb** assembly (CSD code: ABELAU[8]), with the ratio of these two depending on the **res** loading. At 100 mol% **res**, all product existed as **res-tpcb** (Fig. 1a) while at lower loadings, all **res** was bound in **res-tpcb**, and the excess **tpcb** remained unbound. Isolation of pure **tpcb** after the catalytic reactions asks for a solvent-based work-up[28] or sublimation.[29] Similarly, milling **res** and **bpe** in a 1 : 2 molar ratio, yielded only a 1 : 1 co-crystal of **res** and **bpe** (**res-bpe**, CSD code: ABEKUN[8]) and the unreacted **bpe** according to PXRD of the crude reaction mixture. When **res-tpcb** was milled with **bpe** in a 1 : 2 molar ratio, only **res-bpe** and **tpcb** were detected by PXRD, showing the higher stability of **res-bpe** over **res-tpcb**.

In situ Raman monitoring during milling revealed two distinct steps (Fig. 1b). First, the co-crystal **res-bpe** forms within five minutes, evidenced by a blue shift in key Raman bands of **bpe** at 1599 and 1636 cm^{-1} to 1606 and 1646 cm^{-1}. This intermediate was previously shown to form readily under mild conditions.[9] Similar was observed for the mechanochemical formation of the H-bonded assembly of phenylboronic acid and 4,4′-bipyridine.[30] The second, slower step involves the photodimerisation of **bpe** within the co-crystal, as seen by the gradual loss of C=C-related Raman bands at 1646 and 1200 cm^{-1} and the appearance of new bands at 997, 1066, 1101 and 1139 cm^{-1} corresponding to the cyclobutane product (Fig. 1c).

Calculations were used to check the feasibility of formation of various H-bonded assemblies and assign the Raman spectra. Results support the experimental findings and are in line with the available report.[10] Both applied functionals identify the **res-bpe** assembly as the most stable H-bonded assembly (Fig. 2). H-bonding between **tpcb** and **res** to form **res-tpcb** is also favourable, explaining why **res** is observed exclusively as **res-tpcb** after the reaction under catalytic conditions. The **res-bpe** assembly is significantly more stable than **res-tpcb** suggesting that, in presence of the unbound **bpe**, **res-bpe** can regenerate from **res-tpcb**, enabling catalytic turnover.

The catalytic reaction likely involves a series of **bpe**/**tpcb** exchanges accompanied by changes in the H-bonding of **res**. Among the possible pathways, the formation of the most stable supramolecular assembly, the "*closed*" assembly **res-bpe**, should be involved in the preferred pathway. As outlined in Fig. 2, the plausible catalytic cycle begins with photoreaction of **res-bpe** to form **res-tpcb**. Subsequent binding of **bpe** to **res-tpcb** yields the "*open*" intermediate **(res)$_2$(bpe)(tpcb)**, which undergoes transition first to the more stable "*closed*" **(res)$_2$(bpe)(tpcb)** and then to "*open2*" upon binding another **bpe**, and finally closes again to regenerate **res-bpe**, releasing **tpcb** and completing the cycle.

While the route similar to the simplified pathway shown in Fig. 2 likely prevails, alternative routes may also contribute depending on the reaction conditions and the solid-state environment, particularly at low **res** loadings. These include direct photocyclisation in "*open*" assemblies such as "*open1*" or "*open2*", or **tpcb**-to-**bpe** exchange in "*open1*" prior to cyclisation. In these intermediates, **bpe** is positioned similarly as in "*open2*" and, as suggested by previous studies,[32–35] may still engage in the template-assisted reaction. We note that *ex situ* monitoring of the reactions by PXRD and NMR methods showed no unidentified species in crude mixtures preventing further analysis.

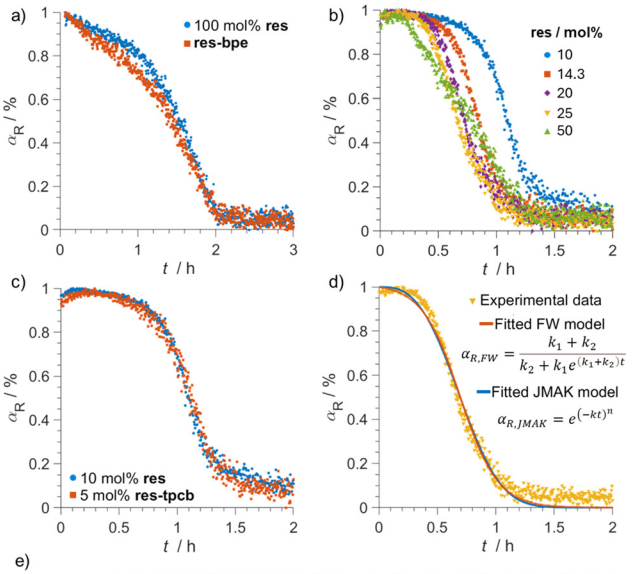

e)

res / mol%	$10^5 \cdot k_1$ / s^{-1}	$10^3 \cdot k_2$ / s^{-1}	R^2_{FW}	n	$10^4 \cdot k$ / s^{-1}	R^2_{JMAK}
50%	7.11	0.921	0.988	1.98	3.09	0.987
25%	2.37	1.69	0.988	2.90	3.52	0.987
20%	1.48	1.77	0.985	3.19	3.31	0.983
14.3%	0.551	1.89	0.989	3.92	2.95	0.985
10%	0.380	1.49	0.980	4.01	2.27	0.976

Fig. 3 Kinetic profiles for **bpe** obtained from *in situ* data for reactions using different **res** loadings: (a) 100 mol% **res** (compared to the reaction of **res-bpe**), (b) 10–50 mol% **res**, and (c) 5 mol% **res-tpcb** (compared to the reaction with 10 mol% **res**). FW (red) and JMAK (blue) analysis: (d) fits using data for 25 mol% **res**, and (e) results according to the equations in (d). Processed Raman data was used for kinetic analysis. Contribution of the PMMA jar was subtracted from the obtained spectra using the most intense PMMA band at 2955 cm^{-1} as a scaling reference. The spectra were truncated to region 1765–930 cm^{-1}. Baseline correction was performed using the ALS algorithm. Normalization was carried out using the l^2 (Euclidian) norm. The Raman band in the region between 1620–1660 cm^{-1} of each spectrum was fitted with a *pseudo*-Voigt function and the area beneath the fitted function was calculated using the trapezoidal rule. Eventual outliers were detected and corrected using a Hampel filter with a window length of 20 data points and a Sigma value of 2. The obtained curves were normalized between 0 and 1 and used for kinetic analysis.

In reactions with equimolar mixtures of **res** and **bpe**, or with pre-formed co-crystals **res-bpe**, the reaction starts quickly due to the (almost) immediate presence of the reactive intermediate. However, some of this intermediate may be trapped inside particles, inaccessible to light.[36,37] This might explain the partially sigmoidal reaction profile of **bpe** determined from Raman changes in the 1620–1660 cm^{-1} region (Fig. 3a). During the first hour, the reaction appears light-limited, resembling first-order behaviour. In the second hour, the reaction accelerates as mechanical action exposes more reaction sites by fracturing particles and continuously generating new reactive surfaces. This can be tentatively connected to grinding as well as to accumulation of stress, strain and defects introduced by formation of the photoproduct.[3,36] These observations align with an earlier report showing that macro-sized **res-bpe** crystals tend to crack under irradiation, whereas smaller micro- or nanometre-sized crystals undergo single-crystal-to-single-crystal (SCSC) transformations.[38]

Ex situ monitoring of repeated irradiation and manual mixing with catalytic **res**-loadings showed an almost linear progression of **bpe** photodimerisation,[10] while the data for the 50 mol% template reaction under vortex conditions was best described by the A2 kinetic model.[12] *In situ* Raman monitoring of our reactions with 10–50 mol% **res** performed in a ball mill revealed characteristic sigmoidal profiles for **bpe** (Fig. 3b). These curves show an initial induction phase with minimal product formation, which becomes significantly longer as the template loading decreases. This is followed by a rapid conversion phase and then a plateau, indicating reaction completion.

The observed sigmoidal kinetics suggests an autocatalytic component, possibly due to the product itself accelerating the reaction. To test this, a control reaction was conducted using 5 mol% of **res-tpcb**. The obtained kinetic profile is highly similar to that of the reaction using 10 mol% of **res** (Fig. 3c). This confirmed that the exchange of bound molecules on the template is fast, and that the induction period is changed more likely due to nucleation and growth processes rather than molecular exchange.

The reaction occurs at supramolecular sites formed by the template. At low **res** loadings, the limited number of active sites slows the reaction. At high loadings, some **res-bpe** assemblies may become inaccessible to light, which may also hinder the conversion. An optimal balance between these effects likely reflects in the fastest reaction using 25 mol% of **res**.

To better understand the solid-state dynamics, the kinetic data for the reactions using catalytic amounts of **res** was fitted using two common models: the Finke–Watzky (FW) and the Johnson–Mehl–Avrami–Kolmogorov (JMAK) models,[26] both previously applied to mechanochemical transformations.[39]

FW modelling (data in red, Fig. 3e) revealed that nucleation (characterized by k_1), which dominates in the initial period, slows with lower **res** loading, likely due to fewer reaction sites. In contrast, the growth phase (characterized by k_2) was faster at lower template concentrations (from 50 to 14.3 mol%), possibly because the limited **res** is more efficiently used at the particle surface. The reaction may benefit from enhanced local concentration of **bpe**, rapid product-template exchange, and mechanical effects such as cracking and fragmentation that expose new reactive surfaces.

JMAK analysis complemented the FW findings (data in blue, Fig. 3e). At 50 mol% **res**, the Avrami exponent n is 2.0, suggesting a 1D process possibly related to growth of the product and/or erosion of product from **bpe** grain surfaces. At 10 mol% **res**, the Avrami exponent increases to 4.0, indicative of random nucleation and 3D growth. This shift suggests that under dilute conditions, the reaction proceeds uniformly across the powder, exploiting random nucleation and unhindered growth, with milling aiding in continuous exposure of fresh surfaces.[12]

The sigmoidal profiles reported here are not due to thermal runaway or "snowballing"[40] effects often seen in highly exothermic or paste-forming reactions. The powders remained free-flowing during milling, and the initial temperature increase was attributed to LED illumination and mechanical agitation, not the reaction itself. No temperature rise was observed during the production phase of the reaction.

In conclusion, this study demonstrates that precise control of the template loading is key to optimizing the kinetics of solid-state olefin photodimerization in a ball mill. Using ball milling and just 10 mol% of the resorcinol template enables clean and stereoselective cyclobutane formation without metal catalysts or solvents that is significantly faster than in the only previously reported work with template loading below 50 mol%.[10] The described fully automated method, with real-time Raman monitoring, is the first to combine low loadings of the template (catalyst) with rapid, quantitative conversion and kinetic analysis. Together, these advances provide a sustainable and efficient solution to long-standing challenges in the solid-state photochemical dimerization of olefins.

Financial support was provided by Croatian Science Foundation (IP-2019-04-9951, IP-2020-02-1419 and DOK-2020-01-7515). We thank Dr Ivica Cvrtila for helpful discussions. Calculations were performed on the Supek supercomputer at SRCE, Zagreb.

Conflicts of interest

There are no conflicts to declare.

Data availability

The data that support the findings of this study are available from the corresponding author upon reasonable request.

Part of the metadata that supports the findings of this study are available in the supporting information (SI) of this article. Supplementary information: detailed experimental procedures, *in situ* Raman monitoring plots, kinetic analysis, spectroscopic characterization data for the obtained compounds, and DFT results. See DOI: **https://doi.org/10.1039/d5cc04696c**.

Notes and references

1 F. Toda, K. Tanaka and A. Sekikawa, *J. Chem. Soc., Chem. Commun.*, 1987, 279–280.
2 S. Poplata, A. Tröster, Y.-Q. Zou and T. Bach, *Chem. Rev.*, 2016, **116**, 9748–9815.
3 S. P. Yelgaonkar and L. R. MacGillivray in *Supramolecular Catalysis, New Directions and Developments*, ed. P. W. N. M. van Leeuwen and M. Raynal, WILEY-VCH, Weinheim, 2022, pp. 401–411.
4 L. R. MacGillivray, G. S. Papaefstathiou, T. Friščić, T. D. Hamilton, D.-K. Bučar, Q. Chu, D. B. Varshney and I. G. Georgiev, *Acc. Chem. Res.*, 2008, **41**, 280–291.
5 M.-M. Gan, J.-G. Yu, Y.-Y. Wang and Y.-F. Han, *Cryst. Growth Des.*, 2018, **18**, 553–565.
6 V. Ramamurthy and J. Sivaguru, *Chem. Rev.*, 2016, **116**, 9914–9993.
7 G. M. J. Schmidt, *Pure Appl. Chem.*, 1971, **27**, 647–678.
8 L. R. MacGillivray, J. L. Reid and J. A. Ripmeester, *J. Am. Chem. Soc.*, 2000, **122**, 7817–7818.
9 M. B. J. Atkinson, D.-K. Bučar, A. N. Sokolov, T. Friščić, C. N. Robinson, M. Y. Bilal, N. G. Sinada, A. Chevannes and L. R. MacGillivray, *Chem. Commun.*, 2008, 5713–5715.
10 A. N. Sokolov, D.-K. Bučar, J. Baltrusaitis, S. X. Gu and L. R. MacGillivray, *Angew. Chem., Int. Ed.*, 2010, **49**, 4273–4277.
11 J. Holdaway, E. Bosch, D. K. Unruh and R. H. Groeneman, *Cryst. Growth Des.*, 2024, **24**, 6101–6104.
12 J. Stojaković, B. S. Farris and L. R. MacGillivray, *Chem. Commun.*, 2012, **48**, 7958–7960.
13 A. A. Colmanet, D. K. Unruh and R. H. Groeneman, *RSC Mechanochem.*, 2025, **2**, 631–635.
14 J. F. Reynes, F. Leon and F. García, *ACS Org. Inorg. Au*, 2024, **4**, 432–470.
15 K. J. Ardila-Fierro and J. G. Hernández, *ChemSusChem*, 2021, **14**, 2145–2162.
16 J. Alić, M. Schlegel, F. Emmerling and T. Stolar, *Angew. Chem., Int. Ed.*, 2024, **63**, e202414745.
17 F. Mele, A. M. Constantin, A. Porcheddu, R. Maggi, G. Maestri, N. Della Ca and L. Capaldo, *Beilstein J. Org. Chem.*, 2025, **21**, 458–472.
18 J. G. Hernández, *Beilstein J. Org. Chem.*, 2017, **13**, 1463–1469.
19 V. Štrukil and I. Sajko, *Chem. Commun.*, 2017, **53**, 9101–9104.
20 D. M. Baier, C. Spula, S. Fanenstich, S. Grätz and L. Borchardt, *Angew. Chem., Int. Ed.*, 2023, **62**, e202218719.
21 S. Biswas, S. Banerjee, M. A. Shlain, A. A. Bardin, R. V. Ulijn, B. L. Nannenga, A. M. Rappe and A. B. Braunschweig, *Faraday Discuss.*, 2023, **241**, 266–277.
22 F. Millward and E. Zysman-Colman, *Angew. Chem., Int. Ed.*, 2024, **63**, e202316169.
23 X. Xin, J. Geng, D. Zhang, H. T. Ang, H. Wang, Y. Cheng, Y. Liu, R. W. Toh, J. Wu and H. Wang, *Nat. Synth.*, 2024, **4**, 177–187.
24 I. Cvrtila, V. Štrukil, M. Alešković, I. Kulcsár, T. Mrla, E. Colacino and I. Halasz, *Chem. Methods*, 2025, **5**, e202400089.
25 S. Lukin, K. Užarević and I. Halasz, *Nat. Protoc.*, 2021, **16**, 3492–3521.
26 M. A. Watzky and R. G. Finke, *J. Am. Chem. Soc.*, 1997, **119**, 10382–10400.
27 J. Vansant, S. Toppet, G. Smets, J. P. Declercq, G. Germain and M. Van Meerssche, *J. Org. Chem.*, 1980, **45**, 1565–1573.
28 T. Friščić, T. D. Hamilton, G. S. Papaefstathiou and L. R. MacGillivray, *J. Chem. Educ.*, 2005, **82**, 1679–1681.
29 B. Zhu, J.-R. Wang, Q. Zhang and X. Mei, *Cryst. Eng. Commun.*, 2016, **18**, 6327–6330.
30 M. Pajić and M. Juribašić Kulcsár, *Chem. – Eur. J.*, 2024, **30**, e202400190.
31 M. J. Frisch, G. W. Trucks, H. B. Schlegel, G. E. Scuseria, M. A. Robb, J. R. Cheeseman, G. Scalmani, V. Barone, G. A. Petersson, H. Nakatsuji, X. Li, M. Caricato, A. V. Marenich, J. Bloino, B. G. Janesko, R. Gomperts, B. Mennucci, H. P. Hratchian, J. V. Ortiz, A. F. Izmaylov, J. L. Sonnenberg, D. Williams-Young, F. Ding, F. Lipparini, F. Egidi, J. Goings, B. Peng, A. Petrone, T. Henderson, D. Ranasinghe, V. G. Zakrzewski, J. Gao, N. Rega, G. Zheng, W. Liang, M. Hada, M. Ehara, K. Toyota, R. Fukuda, J. Hasegawa, M. Ishida, T. Nakajima, Y. Honda, O. Kitao, H. Nakai, T. Vreven, K. Throssell, J. A. Montgomery Jr., J. E. Peralta, F. Ogliaro, M. J. Bearpark, J. J. Heyd, E. N. Brothers, K. N. Kudin, V. N. Staroverov, T. A. Keith, R. Kobayashi, J. Normand, K. Raghavachari, A. P. Rendell, J. C. Burant, S. S. Iyengar, J. Tomasi, M. Cossi, J. M. Millam, M. Klene, C. Adamo, R. Cammi, J. W. Ochterski, R. L. Martin, K. Morokuma, O. Farkas, J. B. Foresman and D. J. Fox, *Gaussian16, Revision C.01*, Gaussian Inc., Wallingford CT, 2016.
32 L. R. MacGillivray, J. L. Reid, J. A. Ripmeester and G. S. Papaefstathiou, *Ind. Eng. Chem. Res.*, 2002, **41**, 4494–4497.
33 D.-K. Bučar, A. Sen, S. V. S. Mariappan and L. R. MacGillivray, *Chem. Commun.*, 2012, **48**, 1790.
34 K. M. Hutchins, J. C. Sumrak and L. R. MacGillivray, *Org. Lett.*, 2014, **16**, 1052–1055.
35 C. Li, D. C. Swenson and L. R. MacGillivray, *Chem. – Eur. J.*, 2022, **28**, e202200978.
36 K. Morimoto, D. Kitagawa, C. J. Bardeen and S. Kobatake, *Chem. – Eur. J.*, 2023, **29**, e202203291.
37 W. Li, T. J. Gately, D. Kitagawa, R. O. Al-Kaysi and C. J. Bardeen, *J. Am. Chem. Soc.*, 2024, **146**, 32757–32765.
38 D.-K. Bučar and L. R. MacGillivray, *J. Am. Chem. Soc.*, 2007, **129**, 32–33.
39 R. J. Allenbaugh, T. M. Ariagno and J. Selby, *RSC Mechanochem.*, 2025, **2**, 30–36.
40 B. P. Hutchings, D. E. Crawford, L. Gao, P. Hu and S. L. James, *Angew. Chem., Int. Ed.*, 2017, **56**, 15252–15256.